Article

Deformation-activated recrystallization twin: New twinning path in pure aluminum enabled by cryogenic and rapid compression

Deformation-Activated Recrystallization Twin

- Cryogenic Impact ~$10^4 s^{-1}$
- Discontinuous DRX
- Orientation Dependent
- CTB-ICTB-CTB Facets

{1 1 1}-CTB
{1 1 2}-ICTB

100 μm

10 μm

polycrystalline

single crystal

77 K   0.5Tm

stress (GPa)   strain rate (s^{-1})

15   15

$\times 10^3$

$1.3 \times 10^4 \ s^{-1}$

0   0

strain   1

Mao Liu, Pengfei Wang, Guoxing Lu, Cheng-Yao Huang, Zhong You, Chien-He Wang, Hung-Wei Yen

pfwang5@ustc.edu.cn (P.W.)
glu@swin.edu.au (G.L.)
homeryen@ntu.edu.tw (H.-W.Y.)

Highlights
Deformation-activated recrystallization twin is enabled by cryogenic impact in pure Al

This new twinning path occurs during discontinuous dynamic recrystallization

Nucleation of these twinning grains prefers boundary edge and corner

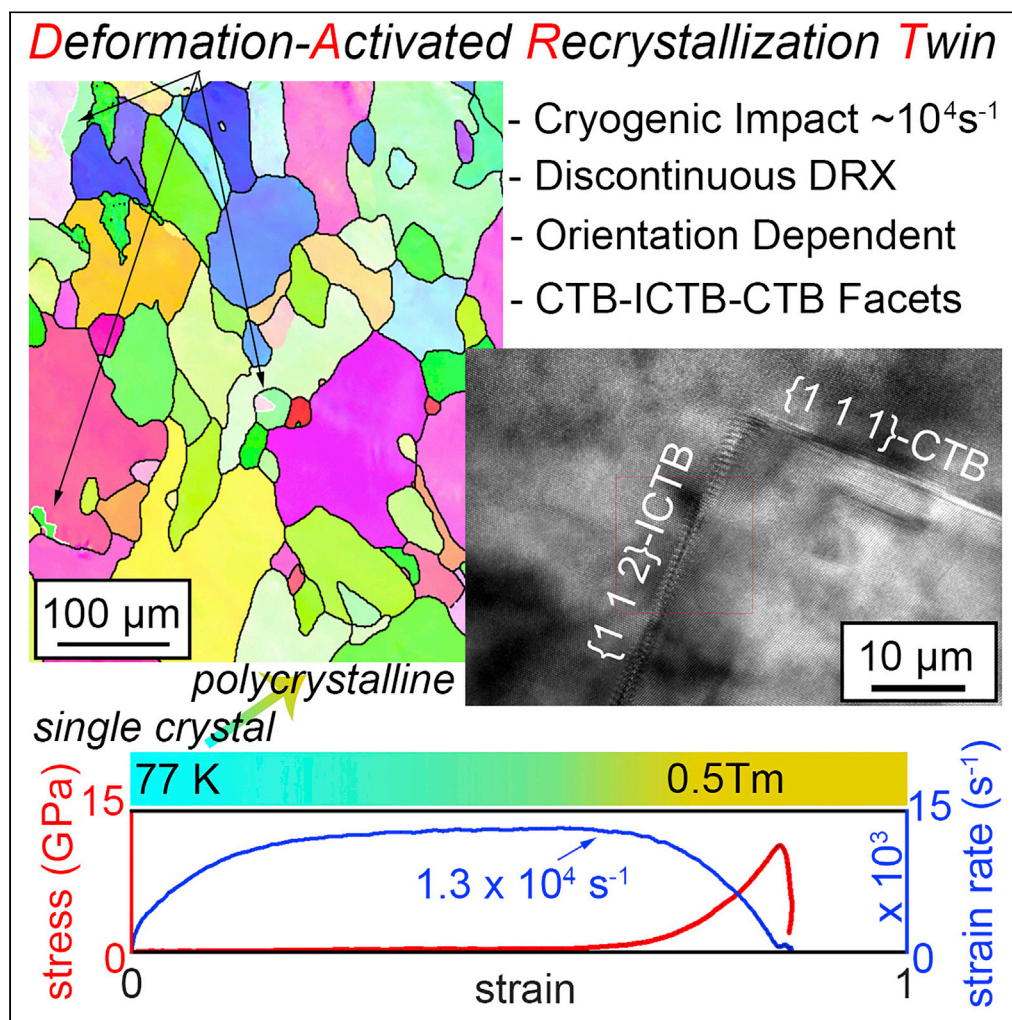Occurrence of new twinning mechanism depends on deformation orientation

Article

Deformation-activated recrystallization twin: New twinning path in pure aluminum enabled by cryogenic and rapid compression

Mao Liu,[1,2] Pengfei Wang,[3,*] Guoxing Lu,[2,*] Cheng-Yao Huang,[4,5] Zhong You,[6] Chien-He Wang,[4,5] and Hung-Wei Yen[4,5,7,*]

SUMMARY

Bulk aluminum rarely forms deformation or annealing twins owing to its high stacking fault energy. We report a novel twinning mechanism mediated by dynamic recrystallization in 6N pure aluminum under high strain rate ($\sim 1.3 \times 10^4 \, s^{-1}$) impact at a cryogenic temperature (77 K). Discontinuous dynamic recrystallization occurs during rapid severe plastic deformation and generates inhomogeneous microstructures exhibiting low-angle and high-angle grain boundaries. Unexpectedly, $\Sigma 3$ twin boundaries were able to develop during dynamic recrystallization. Although these recrystallization twins have similar morphology as that of annealing twins, their formation relies on deformation activation instead of thermal activation, which was suppressed by the cryogenic experiment. Besides, strong orientation dependence was observed for formation of these novel twins. Beyond annealing and deformation twin, deformation-activated recrystallization twin is a new path for pure aluminum twinning.

INTRODUCTION

Based on the formation mechanism, twins can be of two types. Plastic deformation in materials with low stacking fault energy (SFE) produces mechanical twins (or deformation twins), which are accompanied by gliding of partial dislocations (Christian and Mahajan, 1995). Annealing low-SFE materials produce annealing twins owing to incorrect stacking during static recrystallization and grain growth (Carpenter and Tamura, 1926). Generally, low-SFE metals are subjected either directly to heat treatment at high temperatures for grain growth under capillary driving forces or to cold deformation followed by heat treatment to proceed to static recrystallization, which is driven by consumption of stored energy (Bozzolo and Bernacki, 2020; Burke and Turnbull, 1952). Dynamic recrystallization (DRX) of metals during hot deformation also contributes to the formation of twins, mainly by growth accidents during the growth stage of the DRX grains, depending on the driving force for grain boundary migration (Mandal et al., 2012a; b). Conventionally, mechanical twins tend to be lenticular for minimization of strain energy, whereas annealing twins are flat for minimization of grain boundary energy. A recent breakthrough is the fabrication of nanotwinned structures by electrodeposition or other techniques, which provide a unique strengthening mechanism in crystals (Lu et al., 2004, 2009a, 2009b). A nanotwinned structure is defined as a growth twin (a type of annealing twin), which has a flat boundary but nanoscaled twin spacing (Beyerlein et al., 2014). Deformation twins and annealing twins can be easily obtained in low-SFE metals or alloys. However, it is difficult to achieve twinned grains in high-SFE metals, particularly in high-purity ones (the higher the purity, the higher the SFE).

The SFE of pure Al is approximately 104–142 mJ/m^2 (Yamakov et al., 2002b), which causes Al to plastically deform via dislocation gliding instead of deformation twins (Xue et al., 2017; Yamakov et al., 2002b). Even under extreme conditions, deformation twins have never been observed in coarse-grained Al (Bilde-Sørensen and Schiøtz, 2003; Christian and Mahajan, 1995; Gray, 1988; Jacobsen and Schiøtz, 2002). However, molecular dynamics simulations have shown the formation of deformation twins in Al in cases where nm-sized grains are assumed (Jacobsen and Schiøtz, 2002; Yamakov et al., 2002a, 2002b). This has been experimentally confirmed in nanocrystalline ultrathin Al films (Chen et al., 2003) and nanocrystalline Al powders (Liao et al., 2003a, 2003b; Wu et al., 2008) exposed to severe plastic deformation. The nucleation of deformation twins in nanocrystalline Al is because the dominant plastic deformation mode (dislocation

gliding) of coarse-grained Al is suppressed in nanocrystalline grains (Chen et al., 2003; Liao et al., 2003a, 2003b). When the grain size of Al decreases below a critical value (~15 nm), the critical stress for dislocation nucleation becomes higher than that for deformation twins; thus, deformation twins replace dislocation slips as the preferred deformation mode (Chen et al., 2003). However, evidence of deformation twin formation was obtained in pure single-crystal Al when subjected to super high-rate (~1 $\times$ 10^6 s^{-1}) severe plastic deformation (Zhao et al., 2016). Under such extreme conditions, it is impossible to accommodate the applied superhigh strain rate owing to the occurrence of a self-pin, and thus, the strain deficit is supplemented by faster propagating deformation twins.

Annealing twins have been observed in almost all deformed and subsequently annealed face-centered cubic metals with low to medium stacking fault energies, such as Ag (Chuang et al., 2012), Cu (Field et al., 2007), and Ni (Lin et al., 2015), but not in high-purity Al. The only evidence of annealing twins observed in high-purity (5N) Al was that twinned grains nucleated at the corners or edges of the grains when annealed at a high temperature (Humphreys and Ferry, 1996; Murr, 1973), but twin bands parallel to the {1 1 1} plane were found in less pure Al (Fujita, 1955). Although annealing twins are rarely observed in high-purity Al, several recent studies have found annealing twins in the early stages of recrystallization of less pure Al (<5N) and Al alloys (Berger et al., 1983; Xu et al., 2017). To date, annealing twins in high-purity Al formed at ambient or low temperatures (<0.5 melting temperature, known as T_m) have never been reported.

Herein, we report a new twinning mechanism in which Σ3 twin grain boundaries developed during DRX in single-crystal high-purity (6N, 99.9999%) Al under rapid deformation at cryogenic temperatures. Based on the observations and in-depth discussion, it is defined as a deformation-induced recrystallization twin that is different from the principles of deformation or annealing twins.

RESULTS

Recrystallization of 6N Al (1 1 1)-single crystal (SC) was enabled by impact with a split-Hopkinson pressure bar cooled with liquid nitrogen at 77 K (Figure S1A). In the impact, the maximum strain rate reached ~1.3 $\times$ 10^4 s^{-1} (Figures 1A and 1B). The thickness of the single-crystal disk was reduced from 2 mm to ~30 μm (Figure S1B), corresponding to a true strain of 4.2. The temperature change was estimated to be 390 K after deformation (Figure S2), and the peak temperature of the specimen could be raised to 467 K, corresponding to 0.50 T_m (melting temperature).

Electron backscattering diffraction (EBSD) was applied to investigate the deformed microstructure as shown in Figure 1C. After the impact, the single crystal was transformed into polycrystalline Al, indicating a dynamic recrystallization process. Besides, as marked by the squares in Figure 1C, a few twins unexpectedly nucleated at the grain boundary corners or edges in the DRX microstructure of the deformed sample. These Σ3 twin boundaries were confirmed by misorientation profiles. This result was repeatable as demonstrated in another cryogenic impact on (1 1 1)-SC (Figure S3). Therefore, under a high strain rate compression at a low temperature, twinned grains can develop during DRX induced by severe plastic deformation. This has never been reported for high-purity Al because, as mentioned earlier, it is very difficult to form twins in high-purity Al. In this study, the obtained twin was called a deformation-activated recrystallization twin (DART) based on the formation process.

Transmission electron microscopy (TEM) was employed to reveal the deformed microstructure in which both low-angle and high-angle grain boundaries developed during the high-rate compression, as shown in Figure 2A. Analysis of the selected area electron diffraction (SAED) patterns (Figures 2B and 2C) show that M1 and M2 are two grains connected by the high-angle grain boundary of the [3 3 1]/55.5° axis-angle pair. Analyses of Kikuchi patterns (Figures 2D–2G) show that the dislocation cells (a, b, c, and d in Figure 2A) or subgrains with sizes of 2–3 μm are bounded in the M1 grain interior. Therefore, such rapid deformation of single-crystal Al under a suppressed thermal influence can generate polycrystals with dislocations and dislocation cells in the grains. Such a microstructure is not attributed to continuous dynamic recrystallization (CDRX), because the size of recrystallized grains (Figure 1C) was over 50 times larger than that of dislocation cells. Besides, the disorientation of the Σ3 twin boundary is 60°. Such a large misorientation cannot be achieved by cell rotation in CDRX. In fact, CDRX is not a viable concept for deformation in single crystals of Al (McQueen and Kassner, 2004), especially if the purity of Al is higher than 99.999% (5N) (Choi et al., 2013; Yamagata, 1995). It is concluded that the recrystallization in this work during the impact occurred
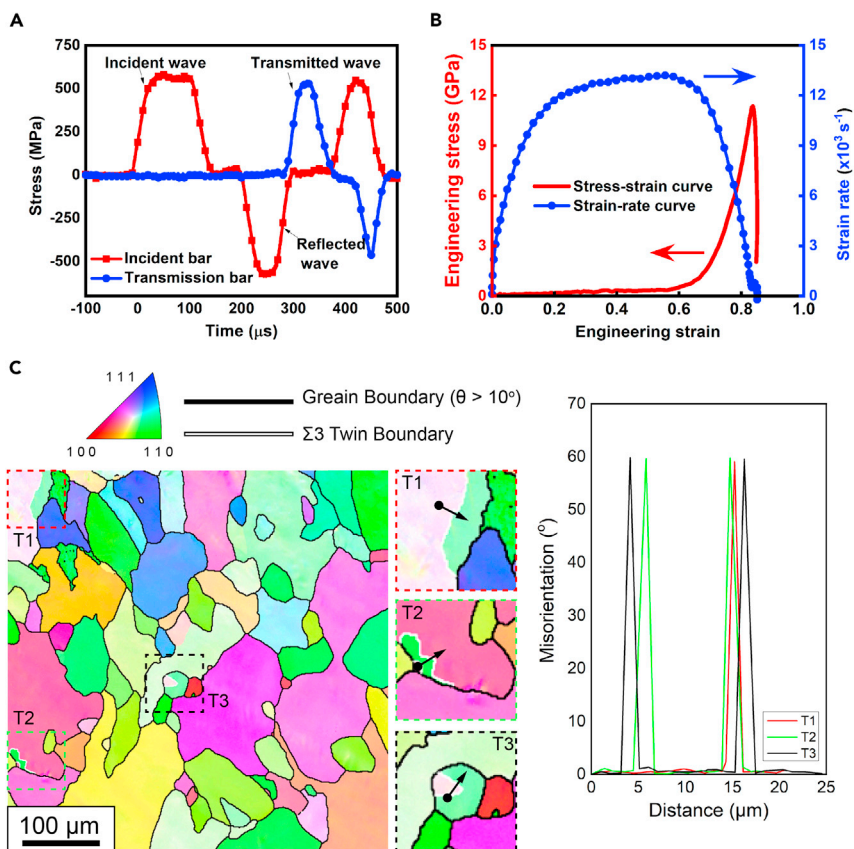
Figure 1. Mechanical and microstructural response of 6N Al (1 1 1)-SC in rapid and cryogenic compression

(A) Three stress waves in Split-Hopkinson pressure bar test under 28 m/s ($\dot{\varepsilon} = 1.3 \times 10^4\ s^{-1}$) impact loading.

(B) Engineering stress-strain curve and strain rate-strain curve.

(C) EBSD-inverse pole figure (IPF)-ND and misorientation profiles across individual twin boundaries.

via discontinuous dynamic recrystallization (DDRX). Typically, DDRX occurs during deformation at a temperature above 0.5 T_m (Sakai et al., 2014), but a study found that DDRX at room temperature is possible in high-purity Al (99.9999%) (Choi et al., 2013). Very high purity, severe plastic deformation, and extremely high strain rates are beneficial for the occurrence of DDRX at low temperatures.

High-resolution TEM (HRTEM) was employed to investigate the detailed structure of these twins, and the results are shown in Figure 3. A recrystallized grain showed a darker contrast, as shown in Figure 3A, and the detailed structure of its corner is magnified in Figure 3B, showing a zigzag-like twin boundary (highlighted by yellow dashed line). The HRTEM image in Figure 3C shows that the ledged grain boundary is composed of a coherent twin boundary (CTB)/incoherent twin boundary (ICTB) junction near the grain corner. The {1 1 2} ICTB is straight and completely perpendicular to the {1 1 1} CTB, as shown in Figures 3D and 3E. This is the first high-resolution observation showing a large CTB-ICTB-CTB structure between twinned grains in a deformed 6N Al single crystal. The CTB-ICTB-CTB ledged structures are the evidence for DDRX because rotation of dislocation cells hardly produces such planar facets. Based on the morphology of the twin (Figure 3), it resembles an annealing twin, because it does not have a lenticular shape, which is a typical feature of a deformation twin. However, annealing twins are not expected in such high-purity 6N Al deformed at such a low temperature without any annealing process. This twinning mechanism is different from previous reports on the formation mechanism of annealing twins in pure Al, that is, the formation of annealing twins in pure Al (5N) with a high-temperature (0.8 T_m) annealing process (Murr, 1973). In this work, twins were attributed to DDRX induced by severe plastic deformation at low temperatures. Therefore, they have been referred to as DARTs. In short, a novel type of recrystallization twin possessing the same morphology as that of an annealing twin can develop in 6N Al under high-rate severe plastic deformation at cryogenic temperatures.
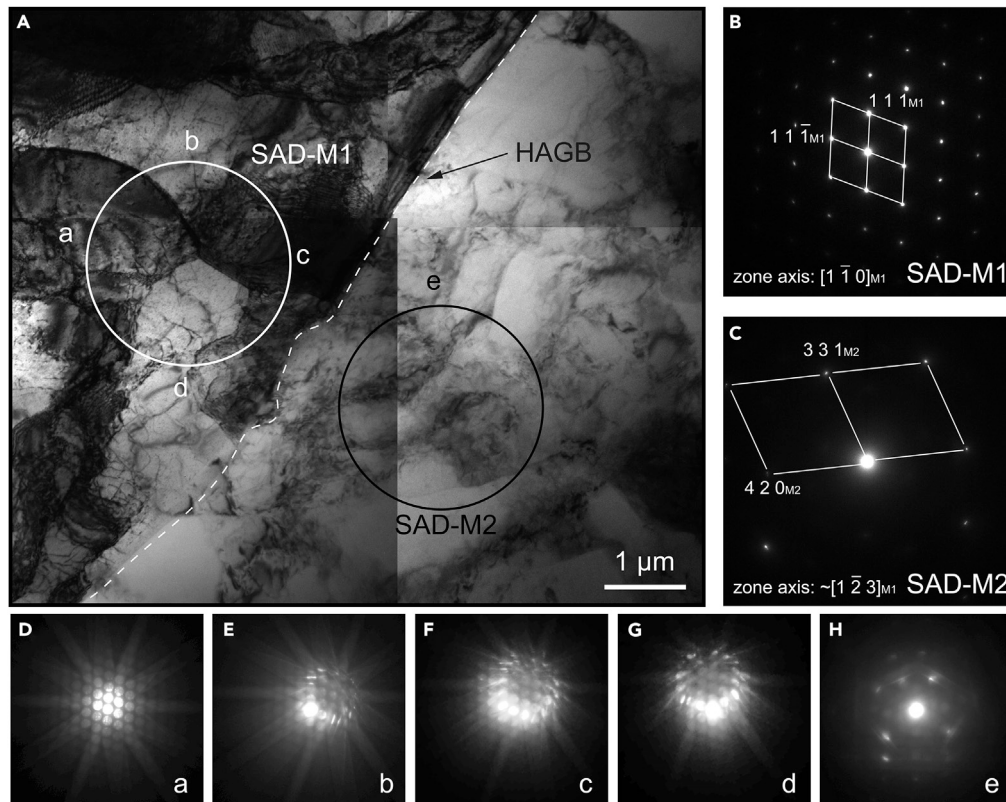
Figure 2. Sub-microstructure of deformed 6N Al (1 1 1)-SC
(A) TEM micrograph showing recrystallization microstructure.
(B) and (C) SAED patterns of the regions highlighted by (A) white and (B) black circles in (A).
(D–H) Kikuchi diffraction patterns of individual subgrains a-e.

The orientation dependence of the twinning mechanism was also examined. Figures 4A and 4B show the microstructure after the rapid and cryogenic impacts in disks with initial NDs//<0 0 1> and <0 1 1>, respectively. Interestingly, no recrystallization twins were observed in the ND//<0 0 1 > sample (Figure 4A). However, more and coarser twins (T1-T4) were observed at the grain boundaries in the ND // <0 1 1> sample, as shown in Figure 4B. Hence, it was concluded that recrystallization twins activated by deformation are orientation-dependent.

To reveal evolution of recrystallization microstructure, a cryogenic compression was done on the ND // <0 1 1> sample at an incident velocity of 5–6 m/s. A true strain of 0.5 is the minimum value that can be achieved without large reduction in strain rate (in one order). As shown in Figure 4C, DDRX still drove the microstructural evolution. Intragranular recrystallization was found: G1 grain held general grain boundary and T1 grain held twin boundary. Both of them kept disorientations larger than 40° with the matrix grain. These results imply that the initial recrystallization of a single crystal can proceed by intragranular DDRX. Although DART can form by intragranular nucleation, intergranular nucleation sites such as boundary edge or corner should be preferred based on our observations.

DISCUSSION

Figure 5A illustrates the formation of DART in cryogenic and rapid compression. The initial recrystallization should proceed by intragranular DDRX, because there is no intergranular site for recrystallization in a single crystal. Once the initial single crystal has recrystallized into polycrystal, DDRX can preferentially nucleate at the grain boundary edge or corner. During this process, DART can form *via* both intragranular and intergranular DDRX. The occurrence of DART depends on crystal orientation and strain rate. This recrystallization behavior is never observed in the previous research.
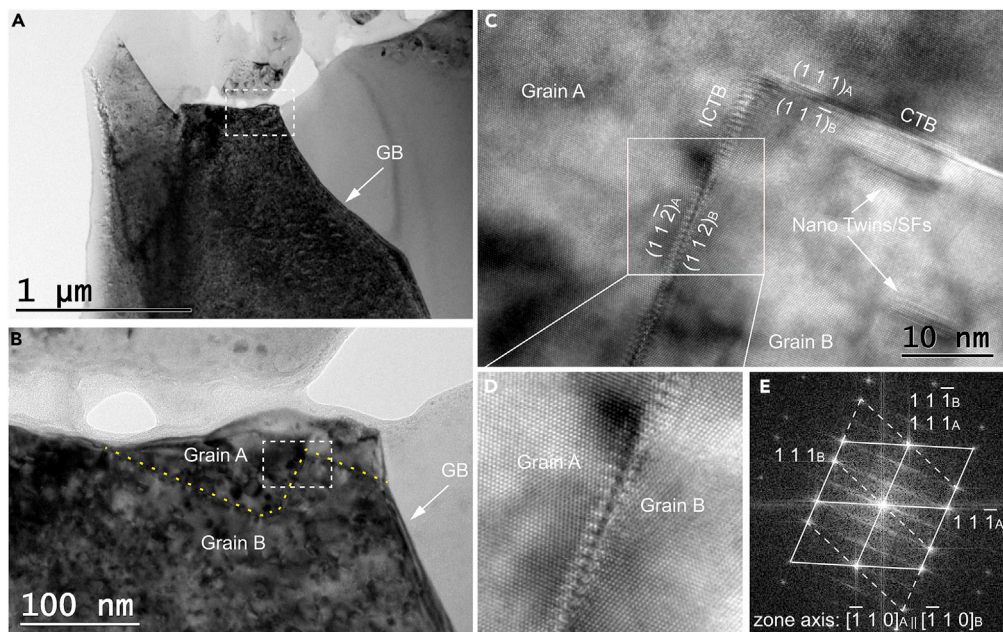
Figure 3. CTB-ICTB-CTB structure in deformed 6N Al (1 1 1)-SC
(A) TEM micrograph showing twinned grains.
(B) Magnified image of the white box in (A) showing a zigzag-like twin boundary.
(C) HRTEM image of the white box in (B) showing a CTB-ICTB junction.
(D) Magnified image of the white box in (C) showing the detailed structure of ICTB.
(E) Diffractogram by fast Fourier transform (FFT) of (D) confirming the $\Sigma 3$ relationship.

Conventionally, three classic models describe the formation mechanism of annealing twins: growth accident model (Carpenter and Tamura, 1926), grain encounter model (Burgers, 1946), and a model involving nucleation of twins by stacking faults or fault packets (Dash and Brown, 1963; Mahajan et al., 1997). All these models are based on the hypothesis that grain boundaries may migrate during annealing. The two main reasons for the migration of grain boundaries during annealing are (Bozzolo and Bernacki, 2020): (a) the migration of a recrystallization front driven by the consumption of energy stored in the form of dislocations that are induced by plastic deformation, and (b) the migration of a grain boundary to reduce its curvature or to adopt a lower energy plane within the so-called grain growth regime with no stored energy involved. Except for the grain encounter model, the aforementioned models involve two different types of twinning mechanisms: (a) the twin is formed by atom addition at wrong sites onto the {111} grain boundary facets, and (b) the twin involves the emission of Shockley partial dislocations at grain boundary ledges/steps as an initiation process (Bozzolo and Bernacki, 2020). In both mechanisms, the grain boundary structure is evoked, indicating that the probability of forming twins is related to the frequency of {1 1 1} facets, which in turn depends on the macroscopic grain boundary plane and local curvature (Bozzolo and Bernacki, 2020). Therefore, the tortuous boundary tends to increase the probability of a suitable configuration along the boundary to nucleate a twin under the activation of deformation. Recrystallization fronts are usually extremely tortuous because of the heterogeneity of the stored energy field, which provides the driving force for their migration. As seen in Figures 1 and 4, most recrystallization fronts, that is, grain boundaries, were tortuous owing to the effects of DDRX.

After nucleation, twins typically grow because of the migration of the noncoherent boundary (Dash and Brown, 1963). The same was observed in this study (Figure 3B and 3C) because the incoherent component of the CTB-ICTB-CTB boundary was responsible for twin growth. Hence, recrystallization twins possessed the same morphology as annealing twins. The annealing twin propensity is allegedly dependent on the migration velocity of the grain boundaries (Mahajan et al., 1997). The applied high strain rate in this study clearly promoted the propensity of recrystallization twinning even in pure Al, because the dislocation generation rate was higher than the dislocation annihilation, which led to an increase in flow stress and consequently increased the propensity of boundary migration. It was evident that there were fewer incoherent
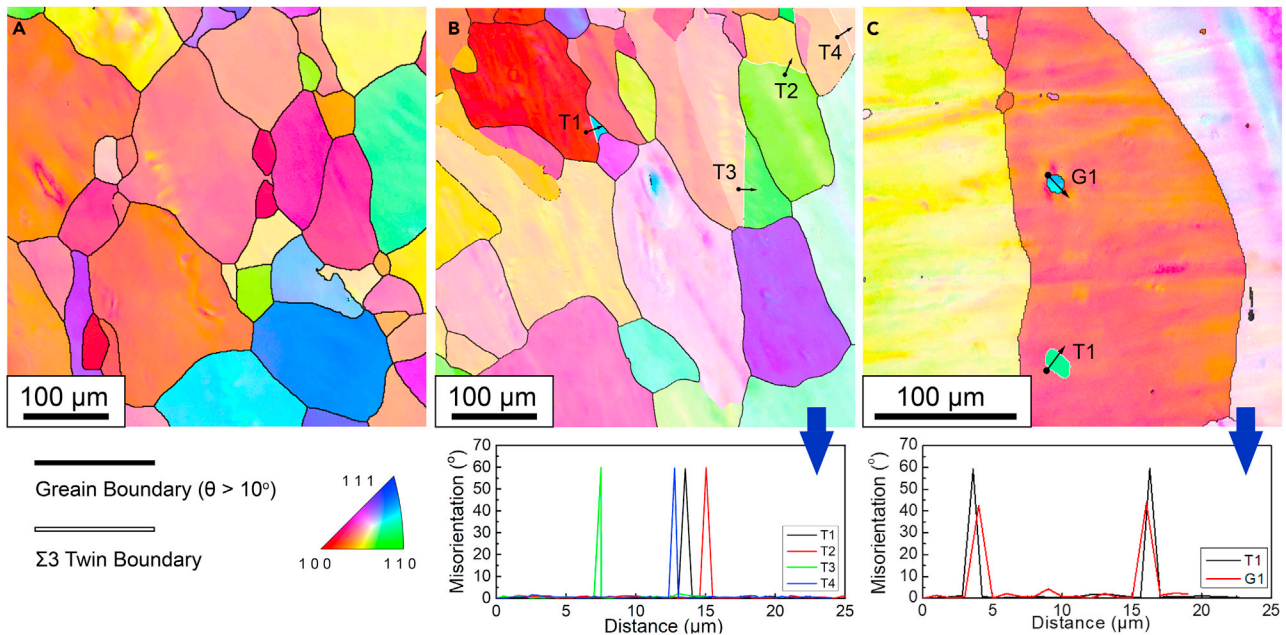
Figure 4. Effects of crystal orientation and strain level on DART in 6N Al SC
(A) and (B) EBSD IPFs-ND of 6N Al (A) (0 0 1)-SC and (B) (0 1 1)-SC.
(C) EBSD IPF-ND of 6N Al (0 1 1)-SC under true strain of 0.5.

facets and longer coherent boundaries after twin growth. In this work, deformation along [1 1 1] produced fine twins, but deformation along [1 1 0] produced coarser twins. The relative orientation between the deformation and crystal gives rise to different migration velocities of the grain boundary (Beck et al., 1950). This, combined with dynamic texture evolution, might be the reason the formation of recrystallization twins depends on the direction of deformation. Therefore, deformation with its strain level, strain rate, and direction is critical to the formation of recrystallization twins.

Figure 5B charts the dynamic twinning response as function of temperature and strain rate in high-purity single crystal or coarse-grained Al. Briefly, an annealing twin appears in Al undergoing static annealing at 0.8 T_m (Murr, 1973) or above (Fujita, 1955). As for the dynamic response, although DDRX can be triggered at a temperature of approximately 0.5 T_m, no twin was observed during DRX (Yamagata et al., 2001). In contrast, deformation twins formed in high-purity Al when the applied strain rate reached $\sim 1 \times 10^6$ s^{-1} (Zhao et al., 2016). On the other hand, no twins (recrystallization or deformations twins) were observed in high-purity Al when the applied strain rate was $\sim 2 \times 10^3$ s^{-1} (Xu et al., 2018). The formation of twins is even more difficult in purer Al (6N Al in this study). As seen in Figure 5B, severe plastic deformation at a high strain rate enabled the breakthrough of twinning, wherein recrystallization twins were activated at the considered temperature. Notably, a deformation rate of 10^6 s^{-1} at room temperature (Zhao et al., 2016) should lead to a larger temperature increase. The formation of deformation twins (Zhao et al., 2016) is explained by the compatibility of plastic kinetics under a super-high strain rate. However, plasticity of deformation twin is not necessary for deformation at the strain rate of 10^4 s^{-1} used in this work. Here, the development of recrystallization twins with DDRX was induced by a much severe strain at a lower temperature. Thus far, this dynamic twinning mechanism has not been reported in pure Al.

Conclusion

High-purity Al is a classic metal that hardly exhibits deformation or annealing twins owing to its high stacking fault energy. The high-strain-rate severe plastic deformation overcomes this challenge in single crystals of 6N Al, even at cryogenic temperatures. During rapid deformation, the single crystal transforms into a polycrystalline microstructure with deformation-induced dislocation substructures. Recrystallization twins with CTB-ICTB-CTB boundary structures nucleate at the grain boundary corners or edges under the activation of severe deformation. It is called a deformation-activation recrystallization twin or DART because its
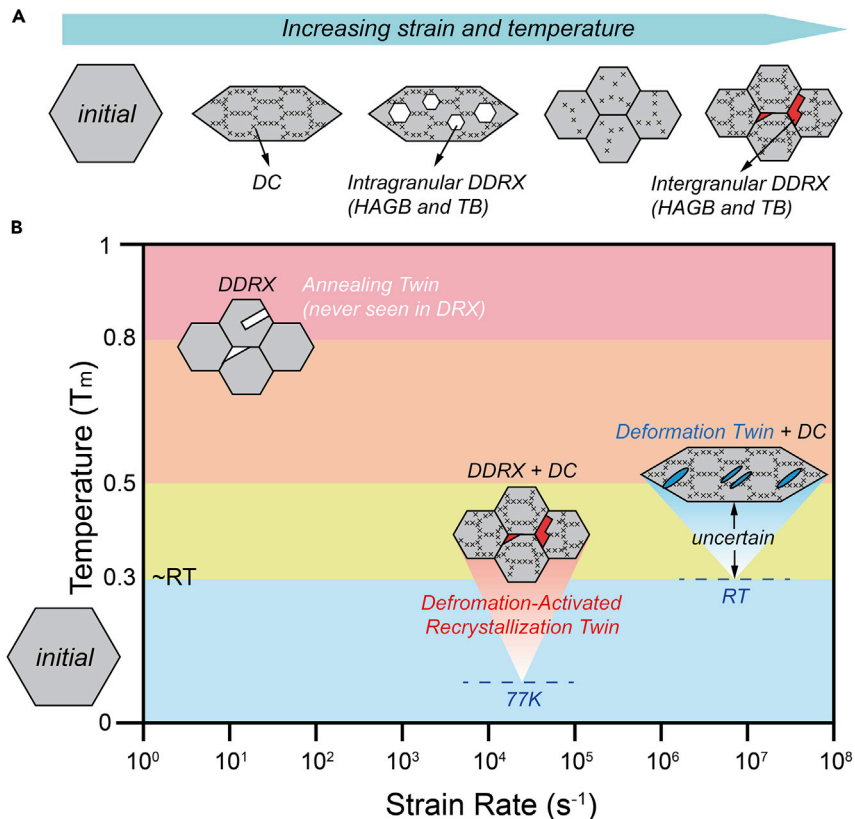
Figure 5. Microstructural responses to cryogenic rapid deformation in pure Al
(A) Microstructural evolution of DDRX and DART.
(B) schematic diagram of the correlation of different types of twinning mechanism: annealing twin (AT), deformation-activated recrystallization twin (DART) and deformation twin (DT), and temperature and strain rate in pure Al.

formation strongly relies on deformation but proceeds *via* a recrystallization process like an annealing twin. In addition, the deformation activation exhibits orientation dependence. This approach opens a new path for twinning in pure Al and other metals with high stacking fault energy.

Limitations of the study

The principles of deformation-activated recrystallization twin might not be applied to materials with low stacking fault energy in which deformation twin *via* motion of partial dislocations will dominate the deformation microstructure. Besides, compression of 6N pure aluminum at an even higher strain rate or beyond cryogenic temperature has not been achieved at this moment.

STAR★METHODS

Detailed methods are provided in the online version of this paper and include the following:

- KEY RESOURCE TABLE
- RESOURCE AVAILABILITY
  - Lead contact
  - Material availability
  - Data and code availability
- EXPERIMENTAL MODEL AND SUBJECT DETAILS
- METHOD DETAILS
  - Materials: 6N Al single crystal
  - Cryogenic impact experiment
  - Transient temperature calculation

- ○ EBSD characterization
- ○ TEM characterizations
- ● QUANTIFICATION AND STATISTICAL ANALYSIS

SUPPLEMENTAL INFORMATION

Supplemental information can be found online at https://doi.org/10.1016/j.isci.2022.104248.

AUTHOR CONTRIBUTIONS

M.L. designed the study; analyzed all the collected data, and wrote the main text. P.W. conducted the impact tests, wrote the supplemental information, and purchased all the Al samples. G.L. supervised the impact tests and revised the manuscript. H-W.Y., C-H.W., and C-Y.H. conducted EBSD and HRTEM characterizations, analyzed the data, and revised the manuscript. Z.Y. revised the manuscript. G.L. and Z.Y. secured the funding for this research.

DECLARATION OF INTERESTS

The authors declare no competing interests.

REFERENCES

Beck, P.A., Sperry, P.R., and Hu, H. (1950). The orientation dependence of the rate of grain boundary migration. J. Appl. Phys. *21*, 420–425. https://doi.org/10.1063/1.1699676.

Berger, A., Wilbrandt, P.J., and Haasen, P. (1983). Development of the recrystallization texture in tensile deformed aluminium single crystals—I. HVEM observations. Acta Metall. *31*, 1433–1443. https://doi.org/10.1016/0001-6160(83)90013-5.

Beyerlein, I.J., Zhang, X., and Misra, A. (2014). Growth twins and deformation twins in metals. Annu. Rev. Mater. Res. *44*, 329–363. https://doi.org/10.1146/annurev-matsci-070813-113304.

Bilde-Sørensen, J.B., and Schiøtz, J. (2003). Nanocrystals get twins. Science *300*, 1244–1245. https://doi.org/10.1126/science.1085577.

Bozzolo, N., and Bernacki, M. (2020). Viewpoint on the formation and evolution of annealing twins during thermomechanical processing of FCC metals and alloys. Metall. Mater. Trans. A *51*, 2665–2684. https://doi.org/10.1007/s11661-020-05772-7.

Burgers, W.G. (1946). 'Stimulation crystals' and twin-formation in recrystallized aluminium.

Nature *157*, 76–77. https://doi.org/10.1038/157076a0.

Burke, J.E., and Turnbull, D. (1952). Recrystallization and grain growth. Prog. Metal Phys. *3*, 220–292. https://doi.org/10.1016/0502-8205(52)90009-9.

Carpenter, H.C.H., and Tamura, S. (1926). The formation of twinned metallic crystals. Proc. R. Soc. Lond. A, Pap. Math. Phys. Character *113*, 161–182. https://doi.org/10.1098/rspa.1926.0144.

Chen, M., Ma, E., Hemker, K.J., Sheng, H., Wang, Y., and Cheng, X. (2003). Deformation twinning in nanocrystalline aluminum. Science *300*, 1275–1277. https://doi.org/10.1126/science.1083727.

Choi, Y.S., Kim, K.I.I., Oh, K.H., Han, H.N., Kang, S.H., Jang, J., and Han, J.H. (2013). Dynamic recrystallization in high-purity aluminum single crystal under frictionless deformation mode at room temperature. J. Mater. Res. *28*, 2829–2834. https://doi.org/10.1557/jmr.2013.265.

Christian, J.W., and Mahajan, S. (1995). Deformation twinning. Prog. Mater. Sci. *39*, 1–157. https://doi.org/10.1016/0079-6425(94)00007-7.

Chuang, T.-H., Wang, H.-C., Tsai, C.-H., Chang, C.-C., Chuang, C.-H., Lee, J.-D., and Tsai, H.-H. (2012). Thermal stability of grain structure and material properties in an annealing-twinned Ag–8Au–3Pd alloy wire. Scripta Mater. *67*, 605–608. https://doi.org/10.1016/j.scriptamat.2012.06.022.

Dash, S., and Brown, N. (1963). An investigation of the origin and growth of annealing twins. Acta Metall. *11*, 1067–1075. https://doi.org/10.1016/0001-6160(63)90195-0.

Field, D.P., Bradford, L.T., Nowell, M.M., and Lillo, T.M. (2007). The role of annealing twins during recrystallization of Cu. Acta Mater. *55*, 4233–4241. https://doi.org/10.1016/j.actamat.2007.03.021.

Fujita, H. (1955). Annealing twin in polycrystalline aluminum. J. Jpn. Inst. Light Met. 52–58. https://doi.org/10.2464/jilm.1955.16_52.

Gray, G.T. (1988). Deformation twinning in Al-4.8 wt% Mg. Acta Metall. *36*, 1745–1754. https://doi.org/10.1016/0001-6160(88)90242-8.

Humphreys, F.J., and Ferry, M. (1996). On the role of twinning in the recrystallization of aluminium.

Scripta Mater. *35*, 99–105. https://doi.org/10.1016/1359-6462(96)00105-4.

Jacobsen, K.W., and Schiøtz, J. (2002). Nanoscale plasticity. Nat. Mater. *1*, 15–16. https://doi.org/10.1038/nmat718.

Li, Y.S., Zhang, Y., Tao, N.R., and Lu, K. (2009). Effect of the Zener–Hollomon parameter on the microstructures and mechanical properties of Cu subjected to plastic deformation. Acta Mater. *57*, 761–772. https://doi.org/10.1016/j.actamat.2008.10.021.

Liao, X.Z., Zhou, F., Lavernia, E.J., He, D.W., and Zhu, Y.T. (2003a). Deformation twins in nanocrystalline Al. Appl. Phys. Lett. *83*, 5062–5064. https://doi.org/10.1063/1.1633975.

Liao, X.Z., Zhou, F., Lavernia, E.J., Srinivasan, S.G., Baskes, M.I., He, D.W., and Zhu, Y.T. (2003b). Deformation mechanism in nanocrystalline Al: partial dislocation slip. Appl. Phys. Lett. *83*, 632–634. https://doi.org/10.1063/1.1594836.

Lin, B., Jin, Y., Hefferan, C.M., Li, S.F., Lind, J., Suter, R.M., Bernacki, M., Bozzolo, N., Rollett, A.D., and Rohrer, G.S. (2015). Observation of annealing twin nucleation at triple lines in nickel during grain growth. Acta Mater. *99*, 63–68. https://doi.org/10.1016/j.actamat.2015.07.041.

Lu, K., Lu, L., and Suresh, S. (2009a). Strengthening materials by engineering coherent internal boundaries at the nanoscale. Science *324*, 349–352. https://doi.org/10.1126/science.1159610.

Lu, L., Chen, X., Huang, X., and Lu, K. (2009b). Revealing the maximum Strength in nanotwinned copper. Science *323*, 607–610. https://doi.org/10.1126/science.1167641.

Lu, L., Shen, Y., Chen, X., Qian, L., and Lu, K. (2004). Ultrahigh Strength and high electrical conductivity in copper. Science *304*, 422–426. https://doi.org/10.1126/science.1092905.

Mahajan, S., Pande, C.S., Imam, M.A., and Rath, B.B. (1997). Formation of annealing twins in f.c.c. crystals. Acta Mater. *45*, 2633–2638. https://doi.org/10.1016/S1359-6454(96)00336-9.

Mandal, S., Bhaduri, A.K., and Subramanya Sarma, V. (2012a). Influence of state of stress on dynamic recrystallization in a titanium-Modified austenitic Stainless Steel. Metallurgical Mater. Trans. A *43*, 410–414. https://doi.org/10.1007/s11661-011-1015-2.

Mandal, S., Bhaduri, A.K., and Subramanya Sarma, V. (2012b). Role of twinning on dynamic recrystallization and microstructure during Moderate to high strain rate hot deformation of a Ti-Modified austenitic Stainless Steel. Metall. Mater. Trans. A *43*, 2056–2068. https://doi.org/10.1007/s11661-011-1012-5.

McQueen, H.J., and Kassner, M.E. (2004). Comments on 'a model of continuous dynamic recrystallization' proposed for aluminum. Scripta Mater. *51*, 461–465. https://doi.org/10.1016/j.scriptamat.2004.05.027.

Mishra, A., Kad, B.K., Gregori, F., and Meyers, M.A. (2007). Microstructural evolution in copper subjected to severe plastic deformation: experiments and analysis. Acta Mater. *55*, 13–28. https://doi.org/10.1016/j.actamat.2006.07.008.

Murr, L.E. (1973). Twin boundary energetics in pure aluminium. Acta Metall. *21*, 791–797. https://doi.org/10.1016/0001-6160(73)90043-6.

Sakai, T., Belyakov, A., Kaibyshev, R., Miura, H., and Jonas, J.J. (2014). Dynamic and post-dynamic recrystallization under hot, cold and severe plastic deformation conditions. Prog. Mater. Sci. *60*, 130–207. https://doi.org/10.1016/j.pmatsci.2013.09.002.

Wu, X.L., Liao, X.Z., Srinivasan, S.G., Zhou, F., Lavernia, E.J., Valiev, R.Z., and Zhu, Y.T. (2008). New deformation twinning mechanism generates zero macroscopic strain in nanocrystalline metals. Phys. Rev. Lett. *100*, 095701. https://doi.org/10.1103/PhysRevLett.100.095701.

Xu, C., Zhang, Y., Godfrey, A., Wu, G., Liu, W., Tischler, J.Z., Liu, Q., and Juul Jensen, D. (2017). Direct observation of nucleation in the bulk of an opaque sample. Sci. Rep. *7*, 42508. https://doi.org/10.1038/srep42508.

Xu, W., Liu, X.C., and Lu, K. (2018). Strain-induced microstructure refinement in pure Al below 100 nm in size. Acta Mater. *152*, 138–147. https://doi.org/10.1016/j.actamat.2018.04.014.

Xue, S., Fan, Z., Lawal, O.B., Thevamaran, R., Li, Q., Liu, Y., Yu, K.Y., Wang, J., Thomas, E.L., Wang, H., and Zhang, X. (2017). High-velocity projectile impact induced 9R phase in ultrafine-grained aluminium. Nat. Commun. *8*, 1653. https://doi.org/10.1038/s41467-017-01729-4.

Yamagata, H. (1995). Dynamic recrystallization and dynamic recovery in pure aluminum at 583K. Acta Metall. Mater. *43*, 723–729. https://doi.org/10.1016/0956-7151(94)00267-L.

Yamagata, H., Ohuchida, Y., Saito, N., and Otsuka, M. (2001). Nucleation of new grains during discontinuous dynamic recrystallization of 99.998 mass% Aluminum at 453 K. Scripta Mater. *45*, 1055–1061. https://doi.org/10.1016/S1359-6462(01)01139-3.

Yamakov, V., Wolf, D., Phillpot, S.R., and Gleiter, H. (2002a). Deformation twinning in nanocrystalline Al by molecular-dynamics simulation. Acta Mater. *50*, 5005–5020. https://doi.org/10.1016/S1359-6454(02)00318-X.

Yamakov, V., Wolf, D., Phillpot, S.R., Mukherjee, A.K., and Gleiter, H. (2002b). Dislocation processes in the deformation of nanocrystalline aluminium by molecular-dynamics simulation. Nat. Mater. *1*, 45–49. https://doi.org/10.1038/nmat700.

Zhao, F., Wang, L., Fan, D., Bie, B.X., Zhou, X.M., Suo, T., Li, Y.L., Chen, M.W., Liu, C.L., Qi, M.L., et al. (2016). Macrodeformation twins in single-crystal aluminum. Phys. Rev. Lett. *116*, 075501. https://doi.org/10.1103/PhysRevLett.116.075501.

STAR★METHODS

KEY RESOURCE TABLE

REAGENT or RESOURCE	SOURCE	IDENTIFIER
Chemicals, peptides, and recombinant proteins		
Methanol/Methyl Alcohol	Katayama Chemical	CAS 64-17-5
Ethanol/Ethyl Alcohol	Nihon Shiyaku Reagent	CAS 67-56-1
Isopropanol/Isopropyl alcohol	Honeywell international Inc.	.CAS 67-63-0
Nitric Acid (61%)	Katayama Chemical	CAS 7697-37-2
Software and algorithms		
OIM Analysis V6	Ametek EDAX	https://www.edax.com/products/ebsd/oim-analysis
OriginLab 2019	OriginLab	https://www.originlab.com/2019
Other		
6N Aluminum Single Crystal Orientation: (100), (110) and (111)	MaTeck GmbH	https://mateck.com/info/aluminium-single-crystal-13al26-9815.html

RESOURCE AVAILABILITY

Lead contact
Further information and requests for resources should be directed to and will be fulfilled by the lead contact, Professor Hung-Wei (Homer) Yen (homeryen@ntu.edu.tw).

Material availability
This study did not generate new materials.

Data and code availability
Data: The data that support the findings of this study are available from the authors on reasonable request. See author contributions for specific datasets.

Code: This paper does not report code.

For any additional questions or information please contact the lead contact.

EXPERIMENTAL MODEL AND SUBJECT DETAILS
This study does not involve experimental model or subject details.

METHOD DETAILS

Materials: 6N Al single crystal
6N Al (99.9999 wt % Al) single crystals (SCs), provided in disc with diameter of 15 mm and height in 2 mm (Φ15 × 2 mm), are commercialized by MaTeck GmbH. The detailed information is listed in Tables S1 and S2 or referred to key resource table. The surface orientations of ordered single-crystal discs include (0 0 1), (0 1 1) and (1 1 1), respectively. A surface orientation of (h k l) means that normal direction (ND) of the disc is parallel to [h k l] and the sample is designated as (h k l)-SC in this study. These single-crystal 6N Al disc were further processed via wire cutting into Φ3 x 2 mm for cryogenic impact experiments.

Cryogenic impact experiment
The low temperature furnace was used to set the target temperature which was controlled by the flow rate of liquid nitrogen vapor. The vapor rate could be self-adjusted by the power of a heating wire inside the liquid Nitrogen bottle as shown in Figure S1A.

The 6N Al single crystal sample was firstly immersed and cooled in liquid Nitrogen for 10 min, then immediately picked up by a tweezer and mounted between the incident and transmission bars (Φ14.5 × 1,000 mm). During the Split-Hopkinson pressure bar (SHPB) test, the projectile (Φ14.5 × 300 mm) was accelerated by the gas along the barrel and impinged the incident bar with a velocity of 28 m/s, generating a compressive stress wave propagating along the incident bar from the impact surface to the sample. A part of the incident wave is reflected to the incident bar as the reflected wave at the interface between the incident bar and the sample, while the other part passes through the sample as the transmitted wave in transmission bar. The incident wave, reflected wave and transmitted wave were measured with normal strain gauges and recorded by an oscilloscope (Tektronix MDO 3024), as shown in Figure 1A. The engineering stress-strain and strain rate-strain curves, as shown in Figure 1B, could be retrieved through processing three waves. The engineering stress could reach 11 GPa with a corresponding maximum strain rate $1.3 \times 10^4 \, s^{-1}$. The final thickness of the deformed sample was measured by field emission scanning electron microscope (ZEISS GeminiSEM 500), as shown in Figure S1B. In the setup for this study, the strain level was unlimited and the true strain was in the rage from 3.9 to 4.2. By reducing impact speed, only one result with controlled strain was shown (Figure 4C) to reveal the effect of strain level.

Transient temperature calculation

Considering the special characterization of the high-rate SPD, the transient temperature rises due to adiabatic heat during deformation can be calculated for 6N Al deformed at cryogenic temperature (77 K in this study):

$$\Delta T = \frac{\beta}{\rho C} \int_{\varepsilon_1}^{\varepsilon_2} \sigma d\varepsilon \qquad \text{(Equation 1)}$$

where β = 0.9 with assumption 90% of work of deformation was converted to heat (Li et al., 2009; Mishra et al., 2007); ρ is the density of Al (2,710 kg/m^3) and C is the specific heat capacity of Al (910 J kg^{-1} K^{-1}). Therefore, the actual sample temperature should be expressed as:

$$T = T_N + \Delta T \qquad \text{(Equation 2)}$$

where T_N is the nominal deformation temperature (77 K in this study). The maximum temperature increment was estimated to be 390 K (Figure S2C) for high-rate SPD process in this study. Therefore, T = 77K + 390 K = 467 K and thus T/T_m is $\sim$0.498.

EBSD characterization

After the cryogenic and rapid compression, the impacted surfaces of Al samples with different initial orientations were mechanically polished first, followed by electropolishing. Specimens for EBSD characterization were prepared by grinding up to 2,500 grids on silicon papers and electrochemically polished at -25°C in a mixture of 25% nitric acid and 75% methanol acid solution with a voltage of 15V for 1.5 min. EBSD was collected by an EBSD detector (manufactured by EDAX) in FEI NOVA NanoSEM450 field-emission gun (FEG) scanning electron microscope (SEM) at 25 kV. Two step sizes was used in this study: 1 μm (Figures 1C, 4A and 4C) and 0.5 μm (Figures 4B and S3). The corresponding data were processed by OIM Analysis V6 software.

TEM characterizations

The TEM foils were prepared. The samples were prepared by a Twin-jet machine using a mixture of 25% nitric acid and 75% methanol acid solution with a voltage of 15V. Focused ion beam (FIB) instrument was not used to fabricate TEM samples in this study, in order to avoid the influences of Gallium ions which may induce microstructural evolution or phase transformation of metallic materials. TEM analyses were performed on FEI Tecnai F20 microscope operated at 200 kV to characterize the microstructural evolution of cross-sectional samples. High-resolution TEM (HRTEM) experiments were also performed to further probe the impact-induced microstructural changes in deformed bulk 6N Al single crystal. It must be noted that nanotwins and stacking faults in TEM/HRTEM images were induced by the exposure of electron beam.

QUANTIFICATION AND STATISTICAL ANALYSIS

This study does not involve quantification or statistical analysis.